RSC Advances

ROYAL SOCIETY OF CHEMISTRY

www.rsc.org/advances

RSC Advances

ARTICLE

A fluorescent biosensor of lysozyme-stabilized copper nanoclusters for the selective detection of glucose

Received 00th January 20xx,
Accepted 00th January 20xx

DOI: 10.1039/x0xx00000x

www.rsc.org/

Chan Wang,[#,a] Shili Shu,[#,c] Yagang Yao*,[b] and Qijun Song*,[a]

Glucose biosensors have attracted increased attention, as the rapid and sensitive detection of glucose is highly desirable for diabetes diagnosis. In this article, we designed a type of lysozyme functionalized fluorescence copper nanoclusters (Lys–CuNCs) to detect glucose levels in blood samples. Fluorescence measurements were carried out to optimize the synthesis conditions (eg. mass ratio, pH and reaction time) for the biosensor. Under optimum conditions, the obtained Lys–CuNCs with an average diameter of 2 nm exhibited bright orangey-red fluorescence with high quantum yields (up to 5.6%). The fluorescence signal of Lys–CuNCs was quenched upon the addition of glucose, presumbly due to the reduction of Cu(I) on the NCs surface by glucose. Thus the Lys-CuNCs can be served as a biosensor for glucose detection and two linear response ranges respectively in 0.03–10 μM and 0.5–10 mM of glucose were observed with a detection limit of 1.9 nM. Furthermore, this biosensor showed superior selectivity for various interferences, including light radiation, metal ions, carbohydrates and amino acids. In view of these properties, the Lys–CuNCs biosensor was applied in the determination of glucose in blood samples, and the results agreed well with that obtained from a currently used clinical method. Finally the visualized fluorescence variation of Lys–CuNCs may further enable the rapid and simple detection of glucose level in blood.

Introduction

Glucose is one of the most important metabolic carbohydrate energy sources, which is crucial to maintaining health. The blood glucose concentration beyond the normal range of 3.1–6.6 mM may cause hyperglycemia (above 6.6) or hypoglycemia (under 3.1).[1,2] Abnormal glucose levels can result in diabetes mellitus, which causes serious health problems including blindness, heart disease, kidney failure and hypertension.[3] Therefore, it is of great significance to monitor glucose levels for diagnosis and treatment of diabetes in a simple, sensitive and efficient way. Since the appearance of the first glucose biosensor in 1962, a lot of effort has been devoted to developing glucose biosensors.[4] Based on the detection method, these biosensors may be classified into colormetry,[5] electrochemistry,[6,7] electrochemiluminescence,[8] and fluorescence method.[9] Among them, fluorescence biosensors became a hotspot in recent years, owing to their operational simplicity, excellent sensitivity, low cost and the availability of multiple signals.

Metal nanoclusters (NCs) have gained great interest because of their unique physicochemical, optical, and electrical properties,[10,11] and thus are widely used in biological imaging,[12,13] catalysis,[14] and chemical sensors.[15–17] In the past decades, metal NCs are one of the most popular fluorescence materials for glucose biosensors. Especially gold nanoclusters (AuNCs) have attracted much attention due to their ultrasmall sizes, bright fluorescence, good biocompatibility and high stability.[18,19] For instance, Xia et al. reported a glucose oxidase (GOD)-functionalized AuNCs as probes for glucose.[20] Radhakumary et al. developed a colormetric probe for glucose using a glucose oxidase/gold nanoparticles bioconjugate.[21] The biomolecule-stabilized AuNCs were also used as a novel fluorescence probe for sensitive and selective detection of glucose.[22]

Compared with Au, the non-precious Cu is earth-abundant and significantly cheaper. CuNCs have also been proved to possess unique photoluminescence (PL) properties, low toxicity and excellent biocompatibility.[10,23] In present work, we developed CuNCs as a fluorescent biosensor for glucose detection. Lysozyme was chosen as template for the preparation of CuNCs, and the fluorescence signals of as-prepared Lys-CuNCs bioconjugates exhibited smart response to the presence of glucose in aqueous solution. This attractive feature enables the CuNCs to serve as probe for glucose-

[a] Key Laboratory of Food Colloids and Biotechnology, Ministry of Education, School of Chemical & Material Engineering, Jiangnan University, Wuxi 214122, China. E-mail: qsong@jiangnan.edu.cn; Tel: +86-510-85917763.
[b] Suzhou Institute of Nano-tech and Nano-bionics, Chinese Academy of Sciences, Suzhou 215123, China. E-mail: ygyao2013@sinano.ac.cn; Tel.: +86-512-62872829.
[c] Department of Chemistry, Tangshan Normal University, Tangshan 063000, China.
† Footnotes relating to the title and/or authors should appear here.
Electronic Supplementary Information (ESI) available: [XPS spectra, FT-IR spectra, Photographs and TEM micrograph of the Lys–CuNCs adding with glucose, and Fluorescence spectra of serum@Lys–CuNCs]. See DOI: 10.1039/x0xx00000x

responsive functional materials. Hence, we explore the utility of the Lys–CuNCs for glucose detection in blood.

Experimental

Materials and apparatus

Lysozyme (CAS number: 12650-88-3, E.C. number: 235-747-3) from chicken egg white was purchased from MP Biomedicals (Irvine, CA). Carbohydrates (eg. glucose, lactose, fructose, sucrose, soluble starch) and amino acids (cysteine, glycine, tryptophan, glutamic acid, lysine, leucine, alanine, proline and methionine) were ordered from Sigma-Aldrich (St. Louis, MO, USA). Copper sulfate ($CuSO_4{\cdot}5H_2O$), sodium hydroxide, hydrazine hydrate ($N_2H_4{\cdot}H_2O$) and ethanol were acquired from Sinopharm Chemical Reagent Co., Ltd (Shanghai, China). All the chemicals were of analytical grade and used as received without further purification. Deionized water was used in all of the experiments.

UV-Vis absorption spectra were recorded with a Lambda 800 spectrophotometer (PerkinElmer, USA). PL experiments were performed with a Shimadzu RF-5301 PC spectrofluorimeter (Shimadzu, Japan) with excitation at 400 nm. X-ray photoelectron spectroscopy (XPS) analysis was performed on a VG ESCALAB MKII spectrometer (ThermoFisher Scientific, USA) with Mg Kα excitation (1,253.6 eV); the binding energy was calibrated with the C 1s band at 284.6 eV. Fourier transform infrared spectroscopy (FT-IR) spectra were recorded in the range of 4000–500 cm^{-1} with a Nicolet Avatar 360 FT-IR spectrophotometer (ThermoFisher Scientific, USA). To study the morphology and estimate the mean diameter of the resultant Lys–CuNCs, transmission electron microscopy (TEM) analyses were conducted on a TECNAI F20 (FEI, USA) operating at an accelerating voltage of 200 kV. Glucose detection was conducted on the blood samples by the standard clinical instrument (Hitachi 7080, Japan) as compared.

Lys–CuNCs Synthesis and optimization

The lysozyme-stabilized CuNCs were prepared by hydrothermal synthesis. To examine the influence of different experimental parameters, we investigated the content of lysozyme ($CuSO_4{\cdot}5H_2O$/lysozyme, mg/mg), the amount of $N_2H_4{\cdot}H_2O$, the pH values of reaction mixture and the reaction time. Here, the reaction time refers to the time after heating up to the required temperature.

In a typical procedure, lysozyme (12.5 mg) and $CuSO_4{\cdot}5H_2O$ (6.4 mg) were added to 5 mL of deionized water under vigorous stirring to produce Lys-Cu ion complex. Then 1 mL of $N_2H_4{\cdot}H_2O$ was introduced to the fully dissolved solution. The mixture was heated to 40 °C under stirring, and the reaction time was 2 h. Subsequently, the NaOH solution (1 M) was added dropwise until a light yellow and transparent solution was obtained, and the corresponding pH was about 12. After cooling to room temperature, the product was collected by precipitating with alcohol and centrifugation at 6,000 rpm. The above purification process was repeated three times. The resultant Lys–CuNCs were freeze-dried under vacuum and stored in a refrigerator for subsequent use.

Glucose detection

Glucose detection in solution. An amounts of 0.2 mL of purified Lys–CuNCs was mixed with various concentrations of glucose (0.03 μM – 1 mM), and then the mixture was diluted to 2 mL with phosphate buffer solution (0.02 M PBS, pH = 7.4). After incubating for 10 min, the fluorescence spectra were recorded with an excitation wavelength of 365 nm. The change in fluorescence intensity was used to construct the calibration curve and evaluate the performance of the resultant Lys–CuNCs.

Interference studies. Various potential interferences, including light radiation, metal ions, carbohydrates and amino acids, were considered to evaluate the selectivity of Lys–CuNCs. This procedure was assayed under the condition identical to those described in glucose detection in solution.

Glucose detection in blood. Samples were collected from healthy persons and the serum was separated from the blood. An ultrafiltration process was conducted to remove large molecules and proteins by using a 3 kDa ultrafiltration tube. Then, 2 mL of treated serum sample was incubated with standard glucose (0.5–17 mM), and diluted 10-fold with PBS. The spiked solution (2 mL) were added to 2 mL of Lys–CuNCs (2 mg/mL) at ambient temperature and the mixture was incubated for 20 min before the variation in fluorescence intensity was monitored at 380 nm.

Results and discussion

Design of Lys–CuNCs biosensor

Owing to the size control ability and the mild reaction conditions,[24] proteins have played an important role in the synthesis of metal NCs, involving bovine serum albumin (BSA),[10,25] insulin,[26] pepsin[27] and lysozyme.[28,29] Lysozyme is an alkaline protein consisting of a single amino acid chain of 129 residues, which are abundant with free carboxyl and amino groups, as well as four disulfide bonds. Such special groups in lysozyme have high affinities with metal ions and facilitate to the formation and stabilization of metal NCs.[30] Thus, we designed a CuNCs biosensor using lysozyme as a template for glucose detection based on the variation in its fluorescence intensity (Scheme 1).

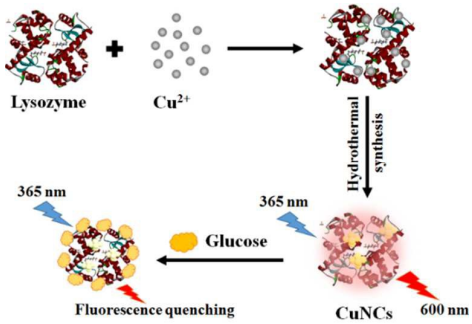

Scheme 1. Schematic diagram of the synthesis of fluorescent lysozyme-stabilized CuNCs and the detection of glucose.

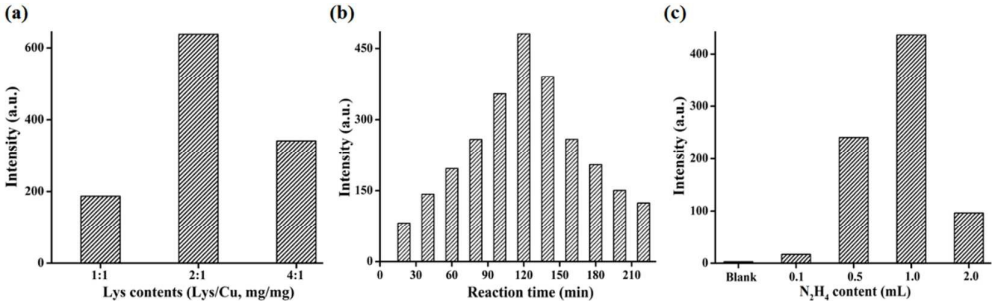

Fig. 1 Effect of (a) lysozyme contents, (b) reaction time, and (c) pH values on the PL intensities at λ_{max} = 600 nm of the resultant Lys–CuNCs.

Three important reaction parameters, i.e., the mass ratio of lysozyme and $CuSO_4 \cdot 5H_2O$ (Lys/Cu), the pH values of reaction solution and the reaction time were optimized to improve the PL intensity of the Lys–CuNCs. The corresponding PL spectra were recorded, and the results are shown in Fig. 1. With the increase of the lysozyme content, the fluorescence intensity increased, reaching the maximum value at Lys/Cu = 2. Once the ratio is exceeded, the free Lys molecules could adsorb on the CuNCs surfaces, causing a decrease in the fluorescence of the Lys–CuNCs (Fig.1 a). As for the effect of the reaction time, the PL intensity increased with the increase of time up to 120 min (Fig.1 b). A prolonged reaction time caused rapid decrease in the PL intensity, suggesting the formation of the non-fluorescent copper nanoparticles.[31] Therefore, we set the reaction time to 120 min. Moreover, it is necessary to control the end-point by monitoring the pH value of the solution. As shown in Fig. 1(c), the highest fluorescence intensity was achieved at the pH value of 12, presumably due to lysozyme turned into a partially unfolded structure that provided larger internal spaces at this pH [32,33]. Such structure helped the formation of more fluorescent CuNCs, resulting in the great increase of PL intensity.

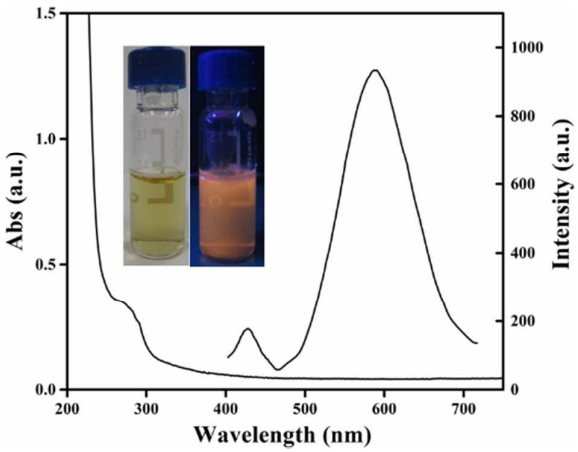

Fig. 2 UV-Vis absorption and emission spectra of the resultant Lys–CuNCs. Inset: photographs of the Lys–CuNCs under the irradiation of visible (left) and UV (right) light.

Characterization of the Lys–CuNCs

According to the above experiments, we synthesized the Lys–CuNCs at 40 °C followed by 120 min incubation with a mass ratio of Lys/Cu=2, maintaining the pH at 12. The UV-Vis and PL spectra of the resultant Lys–CuNCs are shown in Fig. 2. The Lys–CuNCs with good dispersion show a yellow color under ambient light, and a bright orangey-red fluorescence under UV irradiation (see inset of Fig. 2). In addition, the presence of a strong absorption peak below 300 nm and the absence of characteristic surface plasmon resonance of the copper particles both implied the formation of the Lys–CuNCs. Upon excitation at 365 nm, the CuNCs exhibited strong orange emission with a peak centering at approximately 600 nm, whereas a weaker fluorescence in the range of 400–450 nm resulted from the lysozyme. The QY of the Lys–CuNCs was determined to be 5.6%, using rodamine 6G (QYs of 95% in ethanol) as the reference.

The sizes of the Lys–CuNCs were estimated by transmission electron microscope (TEM), and the results are shown in Fig. 3(a). The Lys–CuNCs are uniformly dispersed with an average size of around 2 nm, without visible large metal nanoparticles or aggregation. Moreover, DLS measurement was used to provide sufficient evidence for particle size, and the result showed the average size was 2.6 nm (Fig.S2 a), which was slightly larger than that in TEM images due to the presence of hydrodynamic radius. X-ray photoelectron spectroscopy (XPS) was utilized to determine the oxidation state of Cu in the Lys–CuNCs. As shown in Fig. 3(b), two peaks appear at 932.5 and 952.8 eV, which can be ascribed to the binding energies of the $2p_{3/2}$ and $2p_{1/2}$ electrons of Cu(0), respectively.[34] The absence of the Cu $2p_{3/2}$ satellite peak around 942.0 eV confirms that the Cu(II) electrons are not present.[43] As the binding energy of Cu(0) is only 0.1 eV away from that of Cu(I),[36] it is not possible to exclude the formation of Cu(I), and the valence state of the Cu in CuNCs most likely lies between 0 and +1. The Cu atoms in such tiny clusters were expected to be positively charged, and the presence of Cu(I) could have contributed to the enhancement of both the stability and the PL intensity of the CuNCs, as supported by previous reports.[37–39] The XPS spectra of other elements (i.e., S 2p, C 1s, N 1s and O 1s) are shown in Fig. S1 in the ESM. The formation of CuO/Cu_2O could be excluded by the HRTEM and XRD analysis. As shown in Fig. S2(b), the crystal lattice fringes are 2.05 Å apart which indicates the (111) planes of the metallic Cu, and there

was no other crystal lattices in HRTEM image. Moreover, there was no apparent diffraction peaks in the range of 2θ = 30°–60° as shown in Fig. S2(c). As reported by literatures, the NCs are too small to possess all of the characteristic diffraction peaks of bulk nanoparticles.

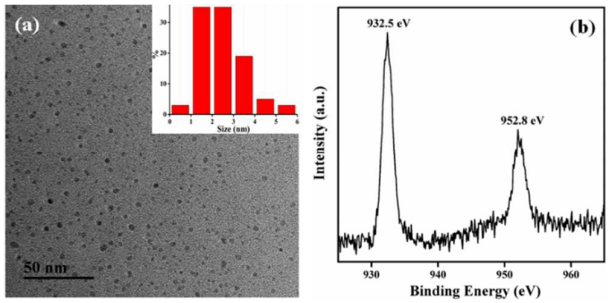

Fig. 3 (a) Transmission electron microscopy (TEM) micrograph (inset: size distribution) of the synthesized fluorescence Lys–CuNCs. (b) X-ray photoelectron spectroscopy (XPS) spectra of Cu 2p in Lys–CuNCs.

The chemical composition of the Lys–CuNCs was further examined by FT-IR measurements (Fig. S3). The absorption band located between 3,330 and 3,400 cm^{-1} is assigned as the absorption peak of the N–H or O–H group, respectively, and the band at 2,960 cm^{-1} is related to C–H stretching. Moreover, lysozyme is a globular protein, and it exhibits a number of characteristic IR absorption bands of protein secondary structures,[40,41] i.e., amide I (C=O stretching vibration, 1645 cm^{-1}), amide II (N–H in-plane bending vibration coupled with C–N stretching vibration, 1527 cm^{-1}) and amide III (1238 cm^{-1}). The peak observed at 2932 cm^{-1} and 2872 cm^{-1} can be assigned to the C–H symmetric and antisymmetric modes, respectively. Owing to the weak absorption of disulfide bonds, their characteristic IR bands cannot be seen in Fig. S3. Moreover, the amide I band showed no discernible shifts, but the peak intensity decreased after assembled to CuNCs, indicating disorder in structure increased and few helical structure were still present.[42,43]

Sensitivity and selectivity of Lys–CuNCs biosensor

To explore the potential application of the obtained Lys–CuNCs for sensing of glucose in blood, we investigated their performance in the aqueous solution. The PL spectra were measured by adding different concentrations of glucose into Lys–CuNCs solutions. By increasing the concentration of glucose from 0.03 μM to 10 mM, the fluorescence intensity of Lys–CuNCs exhibited a gradual decrease at 600 nm (Fig.4 (b)). Moreover, no discernible changes in the maximum peaks or shape of the fluorescence spectrum accompanied quenching, except a slight red shift at higher glucose concentration, as listed in Fig. 4(b). The two different linear relationships of fluorescence intensity versus the glucose concentration are shown in the inset of Fig. 4(c). For glucose concentration from 0.03 to 10 μM, the calibration equation is I = –4.8 C + 662.2 with a correlation efficiency of 0.996, and the detection limit at a signal-to-noise ratio of 3 was estimated to be 1.9 nM.[44] Moreover, a second calibration range can be obtained for the glucose concentration from 0.5 to 10 mM with an equation of I = –0.03 C + 457.4. This detection range covers the normal level (3.1–6.6 mM) of glucose in blood from healthy persons, suggesting the applicability of our Lys–CuNCs as a blood glucose biosensor.

The effect of pH was investigated in order to evaluate the feasibility of fluorescent Lys–CuNCs, and the results were shown in Fig. 4(a). The as-prepared Lys–CuNCs displayed relative high fluorescent intensity in the pH range of 5–9. As shown in Fig. S4(a), the fluorescence intensity of Lys–CuNCs at pH=5 did not respond to the addition of glucose until the concentration up to 0.01 M, suggesting the probe at this pH was not suitable for glucose detection. In contrast at pH 9, the fluorescence intensity of Lys–CuNCs exhibited a gradual decrease with the increase of glucose concentration from 0.01 μM to 0.1 mM (Fig.S4 b and c), but the sensitivity of the sensor was substantially lower than that obtained at the physiological pH 7–8（Fig.4 b and c）. According to the above analysis, the Lys–CuNCs exhibited good applicability as a blood glucose biosensor at the physiologically relevant pH range. The effect of ionic strength was also considered in present work. As shown in Fig. S5, the PL intensity and maximum peaks or shape of Lys–CuNCs did not changed up to the addition of 200 mM KCl or NaCl, which corresponds to the concentration of 0.9% Saline (w.t.). Thus it can be concluded that the Lys–CuNCs showed the high stability, suggesting a promising applicability of the probe for serum analysis.

As we know, the fluorescence quenching follow different mechanisms, (a) exited state reactions, (b) energy transfer, (c) dynamic quenching and (d) static quenching. The last two mechanisms were mainly considered, and the static quenching is usually resulted from the formation of a stable complex between the protein and quencher, while, the dynamic quenching is usually resulted from collisional encounters between the protein and quencher.[45,46] The dependence of PL intensity on the quencher concentration can be used to predict the quenching mechanism.[47–49] This was done by fitting our experimental data to the Stern-Volmer equation (1).

$$\frac{I_0}{I_i} = 1 + K_q \cdot \tau_0 \cdot [Q] \quad (1)$$

where I_0 and I_i are the PL intensity of the Lys–CuNCs in the absence and presence of glucose, respectively, Q is the glucose concentration, τ_0 is the average lifetime of fluorescence molecules in the absence of quencher, and K_q is the dynamic quenching rate constant.

According to the data from Fig. S6, the average lifetime of Lys–CuNCs in the absence of glucose was measured by a picosecond-resolved time correlated single-photon counting (TCSPC) technique. The numerical fitting of the luminescence collected at 495 nm reveals time constants of 2.03 ns (22%) and 8.21 ns (78%), and the average lifetime of Lys–CuNCs is 6.85 ns. After putting it into the equation (1), the K_q is calculated to be 2.2×10^{11} $L\cdot mol^{-1}\cdot s^{-1}$, which is much larger than the constant of Collision-Diffusion between quencher and fluorescence molecules (2×10^{10} $L\cdot mol^{-1}\cdot s^{-1}$),[47] and thus the mechanism can be ascribed to static

quenching, i.e., a ground-state non-fluorescent complex is formed between Lys–CuNCs and glucose. Two factors may be responsible for fluorescence quenching in our hypothesis. First, the oxidized-state Cu(I) on the surface of CuNCs could be reduced to Cu(0) by glucose, of which the mechanism is similar to the silver mirror reaction. The presence of Cu(I) greatly increases the PL intensity of Lys–CuNCs, hence its reduction could cause the quenching fluorescence. In order to further investigate the fluorescence provider in our hypothesis, the fluorescence quenching of pristine lysozyme (without copper) in the presence of glucose was considered, and the result was shown in Fig. S7. Apparently, lysozyme had no response to glucose, which confirmed that the fluorescence signal was belonged to CuNCs provider.

According to the experiments of pH effect, the fluorescence intensity of Lys-CuNCs were highly sensitive to glucose detection in the weakly alkaline or neutral aqueous solution as shown in Figure S4. As reported by references,[50,51] the alkaline condition was helpful for promoting the oxidization of glucose to gluconic acid. Therefore, these results could confirm the detection of glucose followed the redox mechanism. Another possibility could be ascribed to the coordination reaction between the carboxyl groups on the produced gluconic acid (GluC) and Cu(I) in Lys–CuNCs, leading to the subsequent formation of the non-fluorescent GluC@CuNCs.[52] Meanwhile, this complex could have prevented CuNCs from absorption with each other and hence no aggregation occurred. This hypothesis was confirmed by the results shown in Fig. S8. When the 1 mM glucose was added, the color of Lys–CuNCs became lighter than that in inset of Fig. 2. In addition, the solution was still well dispersed with no precipitation, and the size of Lys–CuNCs increased to 4–10 nm after adding glucose, which may prove the formation of the GluC@CuNCs complex.

To investigate the ability of the Lys–CuNCs as sensors for the selective detection of glucose, the interferences of light radiation and metal ions were examined, and the results are shown in Fig. 5. The Lys–CuNCs solution was transferred into a 1 mL quartz cuvette, which was put in the cell holder of spectrofluorimeter with 450 nm Xenon lamp. Fig. 5(a) shows the time evolution of PL intensity of CuNCs during a 120 min light radiation period. Within the investigated duration, Moreover, a variety of metal ions (Na^+, K^+, Zn^{2+}, Fe^{3+}, Ca^{2+}, Mg^{2+}, Cu^{2+}, Cr^{2+}, Pb^{2+}, Cd^{2+}, Co^{2+}, Mn^{2+}, Ni^{2+} and CrO_4^{2-}) were respectively introduced into the Lys–CuNCs solution with pH 7.4 PBS buffer, ensuring the ion concentration at 10 μM. As could be seen in Fig. 5(b), these foreign ions do not lead to any significant fluorescence changes at all.

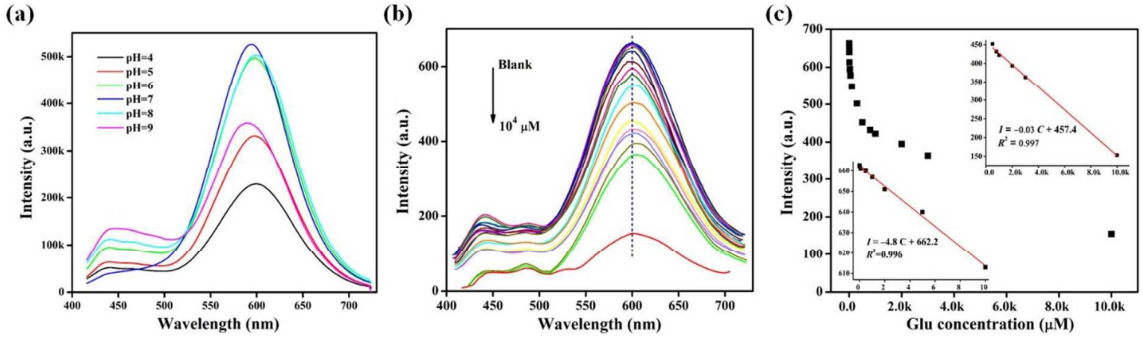

Fig. 4 (a) Effect of pH values on the fluorescence intensity of Lys–CuNCs. (b) Fluorescence spectra of Lys–CuNCs in the presence of different glucose concentrations. The arrows indicate the signal changes as increases in glucose concentrations (0, 0.03, 0.1, 0.5, 1, 2, 5, 10, 25, 50, 100, 300, 500, 800, 10^3, 2×10^3, 3×10^3 and 10^4 μM). (c) Fluorescence intensity at λ_{max} = 600 nm for Lys–CuNCs against the glucose concentrations. Inset: plots of fluorescence intensity vs concentration over two ranges of 0.03–10 μM and 500 μM – 10 mM, respectively.

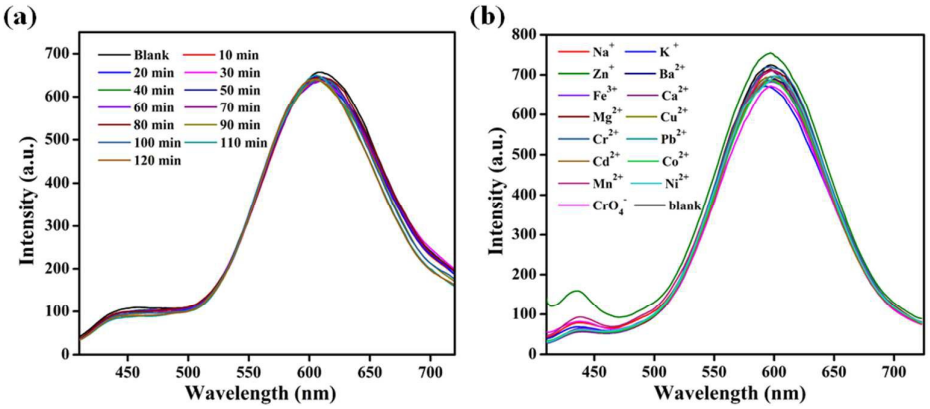

Fig. 5 Fluorescence spectra of Lys–CuNCs measured after (a) light radiation maintaining in different times; (b) the addition of various foreign ions with PBS buffer at pH 7.4. The concentration of each analyte is 10 μM.

Subsequently, the as-prepared Lys–CuNCs were treated respectively with other carbohydrates (eg. lactose, fructose, sucrose, starch solutable) and amino acids (eg. cysteine, glycine, tryptophan, glutamic acid, lysine, leucine alanine, protine and methionine), and the fluorescence intensity rations were recorded. As shown in Fig. 6, the highest value of $(I_0–I)/I_0$ was observed in the case of glucose treatment. The addition of lactose, fructose and cysteine also showed some influence on the fluorescence intensity, whereas the remaining analytes had a negligible effect under identical conditions. These results further illustrated that non-reducing analytes cannot cause the quenching effect on the fluorescence, suggesting the Lys–CuNCs sensors have good selectivity for glucose detection.

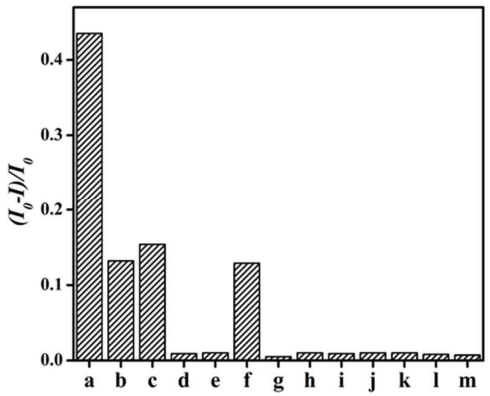

Fig. 6 Relative fluorescence intensity $[(I_0–I)/I_0]$ at 600 nm of Lys–CuNCs in pH 7.4 PBS buffer after the addition of (a) glucose, (b) lactose, (c) fructose, (d) soluble starch, (e) sucrose, (f) cysteine, (g) glycine, (h) methionine, (i) tryptophan, (j) glutamic acid, (k) lysine, (l) alanine, and (m) proline. The concentration of glucose and each analyte are respectively 10 and 100 μM.

Glucose sensing blood samples

To evaluate the feasibility of our proposed method, the Lys–CuNCs sensor was employed to detect glucose in blood samples. A series of blood samples from healthy persons were collected, and the serums were separated from the coagulated blood. The spiked samples were respectively added to the Lys–CuNCs and were incubated for 15 min. The photographs of serum/glucose@Lys–CuNCs complexes are presented in Fig. 7, and the corresponding PL spectra are shown in Fig. S9. As can be seen, the color of all samples look very similar by naked eyes. Under UV irradiation, the pure serum and Lys–CuNCs exhibit blue and bright orangey-red fluorescence, respectively. After adding glucose, the color changed from light orange to pale blue, therefore, it is particularly convenient to detect blood glucose by colorimetric assay, without any complicated instrumentation or operation procedure. Fig. S4 shows that the fluorescence intensity at about 600 nm decreases with the increase of glucose concentration, and these data are similar to that calculated from the second calibration equation as shown in the inset of Fig. 4(b).

According to the above investigations, the good correlation was obtained between the PL intensity and the glucose concentrations, suggesting the feasibility of the use of our method for the quantitative measurement of glucose in blood. To validate the new method, glucose detection was further conducted on the blood samples with unknown concentration levels, and the results were compared with that obtained from the standard clinical method (STM). The glucose levels were quantified using the calibration plot ($I = –0.03\ C + 457.4$), and the results are shown in Table 1. The data obtained by our method are close to that by STM. Hence it is feasible to determination of glucose level in blood by the lysozyme-stabilized CuNCs sensors.

Table 1 Glucose detection in serum samples diluted by 10-flods (n=3)

Sample	Glucose concentration / mM				AVERAGE	SD	RSD / %
	Detection by STM*	Detection by our method					
1	14.1	14	13.7	13.4	13.7	0.3	2.2
2	2.9	2.1	2.2	2.0	2.1	0.1	4.8
3	5.5	4.8	5.1	5.2	5.0	0.2	4.1

* STM: Standard clinical method

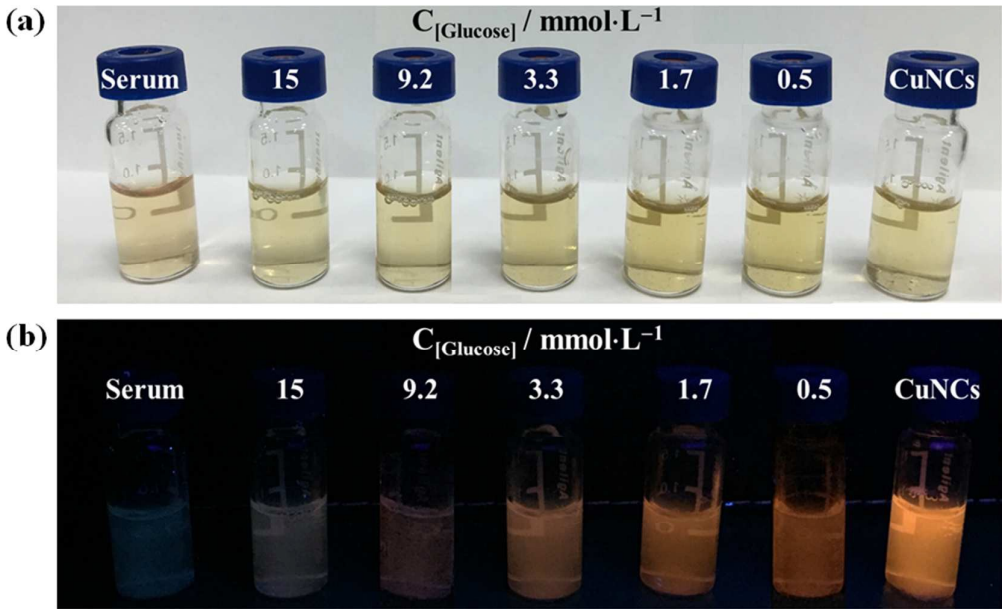

Fig. 7 Photographs of the serum/glucose@Lys–CuNCs for 7 input modes under the irradiation of visible (a) and UV (b) light. The initial serum (first) and Lys–CuNCs (last) samples were used as the control.

Conclusions

We present a convenient method to prepare fluorescence copper nanoclusters using lysozyme as a template. The resultant Lys–CuNCs show a number of remarkable features, including water solubility, bright orangey-red fluorescence, and high quantum yields. Significantly, the PL intensity of Lys–CuNCs is found to be selectively quenched by glucose, and two linear ranges from 0.03 to 10 μM and 0.5 to 10 mM with high sensitivity were obtained for glucose quantification. Meanwhile, the visualization fluorescence variation of Lys–CuNCs may further enable the rapid and simple detection of blood glucose level. Given the attractive fluorescence features, Lys–CuNCs biosensor are quite promising for applications in sensing blood glucose level.

Acknowledgements

This work was supported by Natural Science Foundation of Jiangsu Province, China (No. BK20140392), Natural National Science Foundation of China (NO. 51502115, No. 51372265 and No. 21175060), the Postdoctoral Research Foundation of Jiangsu Province, China (No. 1401058B), the foundation of Key Laboratory of Food Colloids and Biotechnology, Ministry of Education, Jiangnan University (No. JDST 2014–08), and the

Notes and references

1 S. Canivell and R. Gomis, *Autoimmun. Rev.,* 2014, **13**, 403–407.
2 J. Wang, *Chem. Rev.,* 2008, **108**, 814–825.
3 N. A. Calcutt, M. E. Cooper, T .S. Kern and A. M. Schmidt, *Nat. Rev. Drug Discov.,* 2009, **8**, 417–429.
4 Clark, L. C. and C. Lyons, Electrode systems for continuous monitoring in cardiovascular surgery. *Ann. NY Acad. Sci.*, 1962, **102**, 29–45.
5 S. Zhu, X. Zhao, J. You, G. Xu and H. Wang, *Analyst*, 2015, **140**, 6398–6403.
6 F. Kong, S. Gu, W. Li, T. Chen, Q. Xu and W. Wang, *Biosens. Bioelectron.*, 2014, **56**, 77–82.
7 X. Feng, H. Cheng, Y. Pan and H. Zheng, *Biosens. Bioelectron.,* 2015, **70**, 411–417.
8 X. Tian, S. Lian, L. Zhao, X. Chen, Z. Huang and X. Chen, *J. Solid State Electrochem.*, 2014, **18**, 2375–2382.
9 R. Gifford, *ChemPhysChem*, 2013, **14**, 2032–2044.
10 C. Wang, C. X. Wang, L. Xu, H. Cheng, Q. Lin and C. Zhang, *Nanocale,* 2014, **6**, 1775–1781.
11 H. Pei, X. L. Zuo, D. Zhu, Q. Huang and C. H. Fan, *Accounts Chem. Res.,* 2014, **47**, 550–559.
12 Y. Tao, Z. H. Li, E. G. Ju, J. S. Ren and X. G. Qu, *Nanoscale*, 2013, **5**, 6154–6160.
13 C. L. Liu, H. T. Wu, Y. H. Hsiao, C. W. Lai, C. W. Shih, Y. K. Peng, K. C. Tang, H. W. Chang, Y. C. Chien, J. K. Hsiao, J. T. Cheng and P. T. Chou, *Angew. Chem. Int. Ed.,* 2011, **50**, 7056–7060.
14 M. Liang, L. B. Wang, X. Liu, W. Qi, R. X. Su, R. L. Huang, Y. J. Yu and Z. M. He, *Nanotechnology*, 2013, **24**, 245601–245608.
15 Y. Yue, T. Y. Liu, H. W. Li, Z. Y. Liu and Y. Q. Wu, *Nanoscale*, 2012, **4**, 2251–2254.
16 R. Ghosh, A. K. Sahoo, S. S. Ghosh, A. Paul and A. Chattopadhyay, *ACS. Appl. Mater. Interfaces.*, 2014, **6**, 3822–3828.
17 Y. Y. Zhao, Y. X. Ma, H. Li and L. Y. Wang, *Anal. Chem.,* 2012, **84**, 386–395.
18 C. Wang, Y. G. Yao and Q. Song, *J. Mater. Chem. C*, 2015, **3**, 5910–5917.
19 J. B. Liu, M. X. Yu, C. Zhou, S. Y. Yang, X. H. Ning and J. Zheng, *J. Am. Chem. Soc.,* 2013, **135**, 4978–4981.
20 X. D. Xia, Y. F. Long and J. X. Wang, *Analytica Chimica Acta*, 2013, **772**, 81–86.
21 C. Radhakumary and K. Sreenivasan, *Anal. Chem.*, 2011, **83**, 2829–2833.
22 L. Jin, L. Shang, S. Guo, Y. Fang, D. Wen, L. Wang, J. Yin and S. Dong, *Biosens. Bioelectron.,* 2011, **26**, 1965–1969

23 C. Wang, Y. Huang, *Nano,* 2013, **8**, 1350054−1350063.
24 Y. L. Xu, J. Sherwood, Y. Qin, D. Crowley, M. Bonizzoni and Y. P. Bao, *Nanoscale*, 2014, **6**, 1515–1524.
25 J. P. Xie, Y. G. Zheng and J. Y. Ying, *J. Am. Chem. Soc.*, 2009, **131**, 888–889.
26 Y. H. Lin and W. L. Tseng, *Anal. Chem.,* 2010, **82**, 9194–9200.
27 H. Kawasaki, K. Hamaguchi, I. Osaka and R. Arakawa, *Adv. Funct. Mater.,* 2011, **21**, 3508–3515.
28 J. Das and S. O. Kelley, *Anal. Chem.*, 2013, **85**, 7333–7338.
29 W. Y. Chen, J. Y. Lin, W. J. Chen, L. Y. Luo, E. W. G. Diau and Y. C. Chen, *Nanomedicine,* 2010, **5**, 755–764.
30 L. N. Johnson and D. C. Phillips, *Nature*, 1965, **206**, 761–763.
31 C. X. Wang, L. Xu, Y. Wang, D. Zhang, X. D. Shi, F. X. Dong, K. Yu, Q. Lin and B. Yang, *Chem. Asian J.,* 2012, **7**, 1652–1656.
32 T. H. Chen and W. L. Tseng. *Small*, 2012, **8**, 1912–1919.
33 S. Nonose, K. Yamashita, T. Okamura, S. Fukase, M. Kawashima, A. Sudo and H. Isono. *J. Phys. Chem. B*, 2014, **118**, 9651−9661.
34 J. J. Brege, C. E. Hamilton, C. A. Crouse and A. R. Barron, *Nano Lett.*, 2009, **9**, 2239–2242.
35 N. Goswami, A. Giri, M. S. Bootharaju, P. L. Xavier, T. Pradeep, and S. K. Pal, *Anal. Chem.,* 2011, **83**, 9676–9680.
36 W. T. Wei, Y. Z. Lu, W. Chen and S. W. Chen, *J. Am. Chem. Soc.,* 2011, **133**, 2060–2063.
37 Z. T. Luo, X. Yuan, Y. Yu, Q. B. Zhang, D. T. Leong, J. Y. Lee and J. P. Xie, *J. Am. Chem. Soc.,* 2012, **134**, 16662−16670.
38 Z. Luo, V. Nachammai, B. Zhang, N. Yan, D. T. Leong, D. Jiang and J. Xie, *J. Am. Chem. Soc.,* 2014, **136**, 10577−10580.
39 C. X. Wang, Y. Wang, L. Xu, X. D. Shi, X. W. Li, X. W. Xu, H. C. Sun, B. Yang and Q. Lin, *Small,* 2013, **9**, 413–420.
40 G. Thakur and R. M. Leblanc, *Langmuir,* 2009, **25**, 2842–2849.
41 A. Barth, *BBA-Bioenergetics,* 2007, **1767**, 1011–1073.
42 S. K. Das, C. Dickinson, F. Lafir, D. F. Brougham and E. Marsili, *Green Chem.*, 2012, **14**, 1322–1334.
43 D. T. Lu, L. L. Liu, F. X. Li, S. M. Shuang, Y. F. Li, M. M. F. Choi and C. Dong, *Spectrochimica Acta Part A*, 2014, **121**, 77–80.
44 Analytical Methods Committee, *Analyst,* 1987, **112**, 199−204.
45 J. R. Lakowicz, Principles of fluorescence spectroscopy, 3rd ed. Springer: New York, 2006.
46 J. M. Costa-Fernández, R. Pereiro and A. Sanz-Medel, *Trac-Trend Anal. Chem.,* 2006, **25**, 207−218.
47 M. R. Eftink and C. A. Ghiron, *Anal. Biochem.,* 1981, **114**, 199−227.
48 J, R. Lakowicz and G. Weber, *Biochemistry,* 1973, **12**, 4171−4179.
49 F. Mehranfar, A. K. Bordbar and H. Parastar, *J. Photoch Photobio B,* 2013, **127**, 100−107.
50 C. C. Chen, C. L. Lin and L. C. Chen, *Electrochimica Acta,* 2015, **152**, 408−416.
51 N. Fujiwara, S. i. Yamazaki, Z. Siroma, T. Ioroi, H. Senoh and K. Yasuda,*Electrochem. Commun.*, 2009, **11**, 390−392.
52 J. S. Maier, S. A. Walker, S. Fantini, M. A. Franceschini and E. Gratton, *Optic. Lett.,* 1994, **19**, 2062−2064.